

COMMUNICATIONS

Adjustable, Broadband, Selective Excitation with Uniform Phase

Kristin E. Cano, Mari A. Smith, and A. J. Shaka¹

Chemistry Department, University of California, Irvine, California 92697-2025

Received October 1, 2001; revised December 20, 2001

An advance in the problem of achieving broadband, selective, and uniform-phase excitation in NMR spectroscopy of liquids is outlined. *Broadband* means that, neglecting relaxation, any frequency bandwidth may be excited even when the available radiofrequency (RF) field strength is strictly limited. *Selective* means that sharp transition edges can be created between pure-phase excitation and no excitation at all. *Uniform phase* means that, neglecting spin-spin coupling, all resonance lines have nearly the same phase. Conventional uniform-phase excitation pulses (e.g., E-BURP), mostly based on amplitude modulation of the RF field, are not broadband: they have an achievable bandwidth that is strictly limited by the peak power available. Other compensated pulses based on adiabatic half-passage, like BIR-4, are not selective. By contrast, inversion pulses based on adiabatic fast passage can be broadband (and selective) in the sense above. The advance outlined is a way to reformulate these frequency modulated (FM) pulses for excitation, rather than just inversion. © 2002 Elsevier Science (USA)

Key Words: selective pulse; broadband pulse; uniform phase excitation; adiabatic pulse; composite pulse; frequency modulation.

Uniform, controlled transformations of nuclear spin magnetization, beyond that attainable by simple radiofrequency (RF) pulses, are important in many NMR experiments and have been investigated by many groups (1–15). Typically, there are competing concerns or limitations, so that the best pulse in one context may not work well in another. In some cases a particular rotation operator, e.g., $R_x(\frac{\pi}{2}) = \exp(-i\frac{\pi}{2}I_x)$, is desired; in others any transformation $I_z \rightarrow -I_y$ is acceptable, or even $I_z \rightarrow -I_y \cos(\varphi) + I_x \sin(\varphi)$ with φ arbitrary. For high-resolution “survey” experiments, nonuniform performance outside the chemical shift range is of no importance, but in other situations it may be crucial to have some kind of uniform behavior over a desired frequency passband, while exciting little or no signal outside, in the stopband. In cases where destruction of stopband magnetization is not detrimental, either excitation sculpting (13, 14) or “prepulses” (15) can be used to modify either transverse or z -magnetization, respectively, to remove magnetization that is not within the desired passband. Both methods

are extremely flexible, allowing essentially arbitrary profiles to be built up subject to relaxation time constraints. The prepulse method (15) has been in the literature for over 16 years, but has been largely ignored, or independently reinvented, numerous times.

However, in some cases the out-of-band magnetization should not be destroyed, so that a true selective excitation pulse, rather than a magnetization filtering scheme, is required. These pulses are typically less forgiving of pulse miscalibration so that, in addition, the tolerance to the intrinsic RF inhomogeneity produced by the coil in a high-resolution probe, in terms of signal loss, or artifact generation, or both, must be quantified. Furthermore, even excitation sculpting merely *preserves* any preexisting magnetization phase: it cannot *create* pure-phase excitation from z -magnetization over arbitrarily large bandwidths. To do that, some flexibility is required. Luckily, some pulses have a parametric dependence on additional variables (aside from just the pulsewidth) that can allow them to be adjusted smoothly for different ranges of operation, for example sharpening the transition between passband and stopband while keeping the pass bandwidth fixed: these are, effectively, an entire family of pulses. Other pulses, like most composite pulses, for example, have a fixed passband/transition aspect ratio that depends on the pulsewidth, T_p , so that altering the latter is tantamount to searching for a different composite pulse altogether. In most cases, frequency-modulated (FM) pulses fall into the former category, while amplitude-modulated pulses and simple composite pulses fall into the latter.

The hyperbolic secant (HS) inversion pulses, initially described in the context of optical spectroscopy (16), were first introduced into the NMR literature, along with the closely related tangential frequency-sweep pulses, by the careful analysis of Pines and co-workers (17, 18). Subsequently they have been exploited for a whole host of very useful applications (19–22). The HS inversion pulses are an example of a family of pulses that are both broadband and selective when it comes to population inversion. *Broadband* in this context means that, for an ensemble of isolated spins neglecting relaxation, any frequency inversion bandwidth can be achieved while keeping the RF field, B_1 , fixed. *Selective* means that, under the restrictions above, the transition

¹ To whom correspondence may be addressed. E-mail: ajshaka@uci.edu.

between passband and stopband can be made arbitrarily narrow. In the case of the HS inversion pulse, essentially any bandwidth can be achieved by adjusting the pulsewidth and range of frequency sweep appropriately, while still maintaining the adiabatic condition (23) that ensures good inversion. To narrow the transition region, and thereby improve selectivity, the pulsewidth can be increased, while keeping the range of frequency sweep constant. These characteristics are not the exclusive bailiwick of the HS inversion pulses, being shared by a whole host of smooth amplitude shapes and associated frequency sweeps (21, 22).

The reason there are many kinds of adiabatic inversion pulses, many with selective profiles, and a dearth of any corresponding excitation pulses, is easy to understand: the phase properties of FM pulses are usually poor, leading to badly behaved spectra. In multidimensional NMR, in particular, where such pulses might be useful, the presence of any out-of-phase resonance makes identification of nearby peaks tedious. For inversion pulses, in contrast, the transformation $I_z \rightarrow -I_z$ is insensitive to any z -rotations. Furthermore, transverse magnetization can be refocused, independent of any pulse-dependent phase shifts, simply by using a pair of identical 180° pulses. This principle was rigorously demonstrated by Levitt and Freeman (1) for the specific case of B_1 -dependent phase shifts caused by simple composite inversion pulses, and stated by Conolly *et al.* for the specific case of adiabatic inversion pulses (24). The general case can be proven easily. Suppose R inverts z -magnetization. Then without loss of generality

$$R = R_z(\varphi_1)R_x(\pi)R_z(\varphi_2) \quad [1]$$

with φ_1 and φ_2 arbitrary phase factors depending on offset, B_1 , any delays, variations in B_0 , etc., and

$$\begin{aligned} RR &= R_z(\varphi_1)R_x(\pi)R_z(\varphi_2)R_z(\varphi_1)R_x(\pi)R_z(\varphi_2) \\ &= R_x(\pi)\{R_{-x}(\pi)R_z(\varphi_1)R_x(\pi)\}R_z(\varphi_2)R_z(\varphi_1)R_x(\pi)R_z(\varphi_2) \\ &= R_x(\pi)R_{-z}(\varphi_1)R_z(\varphi_2)R_z(\varphi_1)R_x(\pi)R_z(\varphi_2) \\ &= R_x(\pi)R_x(\pi)\{R_{-x}(\pi)R_{-z}(\varphi_1)R_z(\varphi_2)R_z(\varphi_1)R_x(\pi)\}R_z(\varphi_2) \\ &= R_x(2\pi)R_z(\varphi_1)R_{-z}(\varphi_2)R_{-z}(\varphi_1)R_z(\varphi_2) \\ &= R_x(2\pi) \end{aligned} \quad [2]$$

completely independent of φ_1 and φ_2 . The proof hinges on the assumption that R inverts perfectly. When R does not invert perfectly, a deeper analysis shows that the phase errors may still be completely canceled, although an amplitude loss will emerge (13, 14) and either pulsed field gradients or phase cycling must be employed to eliminate magnetization from spins that are not “flipped.” Of course $R_x(2\pi)$ is not the desired transformation—rather $R_x(\pi)$ is. The answer to this objection is that any spin echo sequence $\tau-R-\tau$ may be replaced with the “double echo” sequence $\tau_1-R-\tau_1-\tau_2-R-\tau_2$. As the delay $\tau_1 \rightarrow 0$ the first inversion element may be considered part of any preceding excitation

pulse, its only role being to prepare transverse magnetization with the correct phase for the second inversion pulse, to produce the best possible echo. This sequence will not, on its own, invert z -magnetization, but simply R alone is sufficient for that. As such, there is no major problem implementing arbitrary FM inversion pulses (25) in common pulse sequences.

It is clearly not possible to assemble the same proof with the starting excitation pulse

$$P = R_z(\varphi_1)R_x\left(\frac{\pi}{2}\right)R_z(\varphi_2), \quad [3]$$

although any such proof not using fictional “inverse” pulses (4–6, 12), if somehow located, would probably be of general interest. Without any general scheme, and anticipating the spirit of several constituent flawed pulses leading to a less flawed whole, it is useful to adopt a more specific model for the HS pulses.

The functional form of the HS pulses is well known (16), with a symmetric hyperbolic secant amplitude profile and anti-symmetric hyperbolic tangent frequency sweep (sech/tanh in common parlance), extending in principle to $\pm\infty$. In practice, of course, the pulse waveform is terminated at some finite time. One parameter, β , controls the level of truncation, typically 1%, of the finite-pulsewidth amplitude function. Another, f_{max} , controls the full range of the frequency sweep. The pulsewidth, T_p , peak field B_1^{peak} , and overall phase of the pulse, $\varphi(0)$, round out the control variables. In terms of these variables, fixing $\text{sech}(\beta) = 0.01$ for simplicity, and understanding that $-\frac{T_p}{2} \leq t \leq \frac{T_p}{2}$,

$$\varphi(t) = \varphi(0) + \varphi_0 \ln \left[\cosh \left(\frac{10.6t}{T_p} \right) \right], \quad [4]$$

$$\omega_1(t) = \gamma B_1^{peak} \text{sech} \left(\frac{10.6t}{T_p} \right) \quad [5]$$

with

$$\varphi_0 = \frac{\pi f_{max} T_p}{10.6} \quad [6]$$

and

$$\frac{\gamma B_1^{peak}}{2\pi} = \kappa \sqrt{\frac{f_{max}}{T_p}}, \quad [7]$$

with κ a number of order unity with a role that will become apparent. In the above formulas f_{max} has units of Hz while t and T_p are in seconds; φ_0 and $\varphi(0)$ are in radians and $\omega_1(t)$ is in rad/s. Equation [7] is only approximate, but is quite accurate as long as $f_{max} \gg T_p^{-1}$, i.e., substantial frequency modulation, a situation we will denote as the *far field* case.

The HS 180° pulse gives excellent inversion independent of B_1^{peak} once B_1^{peak} is strong enough. Choosing $\kappa = 1.83$ gives

good results in the far field case. However, if $B_1^{peak} = 0$ then clearly no inversion can occur. It follows that there is a (non-adiabatic) condition at which $I_z \rightarrow 0$ if B_1^{peak} is deliberately reduced. These “HS 90°” pulses have strong phase rolls over their operating bandwidth, but maintain the uniform selective profile of their 180° cousins, a fact that has been independently recently observed in experiments in which simple destruction of z -magnetization is the goal (26). Figure 1 shows the expected

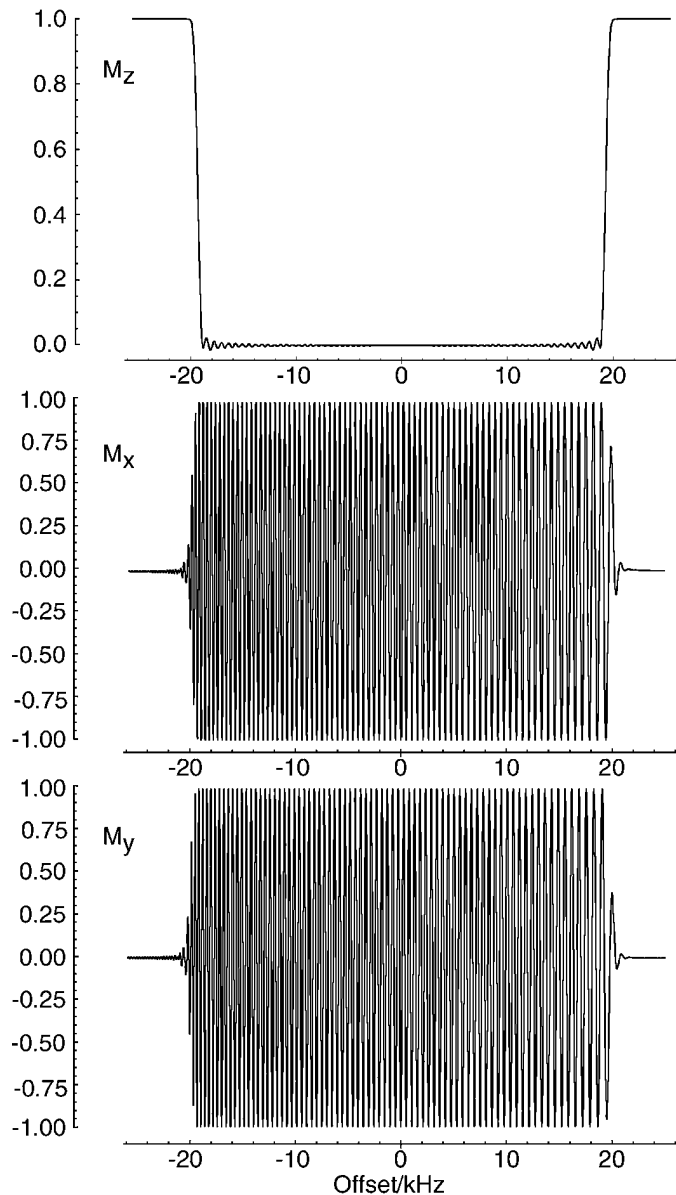


FIG. 1. The calculated z -, x -, and y -magnetization immediately following a 4.0 ms HS 90° pulse applied to equilibrium magnetization, as described in the text. The z -profile shows nearly uniform destruction of magnetization over the passband and sharp transitions to the stopband. Unfortunately, the other two components show violent phase behavior as a function of offset, consisting of a large linear phase correction and a smaller quadratic correction.

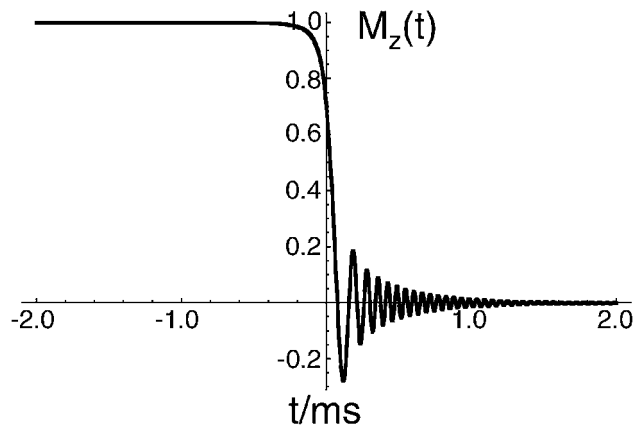


FIG. 2. The calculated time dependence of the z -component of magnetization for a spin in the center of the passband that is subjected to the 4.0 ms HS 90° pulse used to produce the offset dependence shown in Fig. 1. During almost the entire first half of the pulse the magnetization remains undisturbed, and is then rapidly excited. Transient oscillations occur as the sweep continues past. They are closely related to the “ringing” observed in early slow passage NMR experiments using magnetic field sweeps.

z -, x -, and y -magnetization, as a function of offset, for a properly calibrated 4-ms HS 90° using a weak *peak* field of only $\gamma B_1^{peak}/2\pi = 1.88$ kHz, and $f_{max} = 38$ kHz, $\kappa = 0.61$. A bandwidth of over 37 kHz is achieved, and the edges reflect the very sharp turnoff that is a known characteristic of the corresponding HS 180° pulses. The phase roll is *mostly* linear, corresponding to a delay of close to half the pulsewidth, but with a period that clearly lengthens from left to right across the bandwidth. Figure 2 clarifies this behavior by following the time-dependence of the z -magnetization for a single on-resonance trajectory. The spin remains mostly unaffected until nearly halfway through the pulse, when the sweep reaches resonance. There follow some transient oscillations in the z -magnetization that are reminiscent of the “ringing” observed in early slow passage experiments (27). Off-resonance trajectories are very similar, with a time shift that reflects the moment when the sweep passes through. As the sweep is approximately linear over the most intense portion of the pulse, the time shift should be roughly proportional to the resonance offset, $\Delta\omega$. Once the overall phase of the HS 90° is adjusted, the rotation operator on resonance must, in fact, be $R_x(\frac{\pi}{2}) = \exp(-i\frac{\pi}{2}I_x)$. This follows from the observation that $I_z = 0$ combined with the proof of Tycko *et al.* (28) that any time-symmetric series of rotation operators, each of which has an axis in the xy -plane, has an overall axis in the xy -plane. Therefore, an approximate working model of the HS 90° pulse is that shown in Fig. 3a. The model also captures important aspects of the HS 180° case, Fig. 3b, although with one major omission that will become clear below. Related models for FM inversion pulses have been employed to rationalize the behavior of such pulses in heteronuclear NMR experiments, where the phase properties of the inversion pulse are unimportant but the timing of the spin flip influences the results (29, 30).

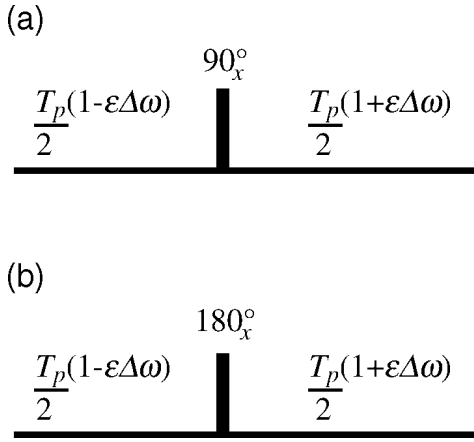


FIG. 3. Simplified models for frequency modulated selective excitation and inversion pulses. A perfect δ -pulse of either 90° or 180° flip angle is sandwiched between two offset-dependent delays. (a) The model for the HS 90° pulse is reasonably adequate providing that the RF field is not too inhomogeneous. (b) The model for the HS 180° is only adequate when a relatively small spatial region of high RF homogeneity is considered. For the more general case, fictitious B_1 -dependent z -rotations should be included, as described in the text.

These simplified models easily explain earlier observations by Hallenga and Lippens (31), found by numerical simulation, that the HS 180° pulse produces a quadratic phase roll when used to refocus transverse magnetization:

$$\begin{aligned}
 R &= R_z\left(\frac{\Delta\omega T_p}{2}(1 + \varepsilon\Delta\omega)\right)R_x(\pi)R_z\left(\frac{\Delta\omega T_p}{2}(1 - \varepsilon\Delta\omega)\right) \\
 &= R_x(\pi)\left\{R_{-x}(\pi)R_z\left(\frac{\Delta\omega T_p}{2}(1 + \varepsilon\Delta\omega)\right)R_x(\pi)\right\} \\
 &\quad \times R_z\left(\frac{\Delta\omega T_p}{2}(1 - \varepsilon\Delta\omega)\right) \\
 &= R_x(\pi)R_{-z}(\varepsilon\Delta\omega^2 T_p). \tag{8}
 \end{aligned}$$

The algebraic sign of the quadratic phase roll depends on the sense of the frequency sweep. How are we to compare the phase roll between the HS 90° and HS 180° pulses? The answer is that ε should be nearly independent of the net flip angle as long as we are in the far field limit and f_{max} is identical. This immediately suggests the following broadband, pure-phase, selective excitation sequence: $P_1 = \text{HS } 90_x^\circ(T_p) - \text{HS } 180_y^\circ(\frac{T_p}{2}) - \frac{T_p}{2}$. All pulses have the same f_{max} including algebraic sign. The transformation achieved is $I_z \rightarrow -I_y$. The analysis parallels that of Eq. [8].

$$\begin{aligned}
 P_1 &= R_z\left(\frac{\Delta\omega T_p}{2}\right)R_z\left(\frac{\Delta\omega T_p}{4}(1 + \varepsilon\Delta\omega)\right) \\
 &\quad \times R_y(\pi)R_z\left(\frac{\Delta\omega T_p}{4}(1 - \varepsilon\Delta\omega)\right)R_z\left(\frac{\Delta\omega T_p}{2}(1 + \varepsilon\Delta\omega)\right) \\
 &\quad \times R_x\left(\frac{\pi}{2}\right)R_z\left(\frac{\Delta\omega T_p}{2}(1 - \varepsilon\Delta\omega)\right)
 \end{aligned}$$

$$\begin{aligned}
 &= R_y(\pi)R_{-z}\left(\frac{\Delta\omega T_p}{2}\right)R_{-z}\left(\frac{\varepsilon\Delta\omega^2 T_p}{2}\right) \\
 &\quad \times R_z\left(\frac{\Delta\omega T_p}{2}(1 + \varepsilon\Delta\omega)\right)R_x\left(\frac{\pi}{2}\right)R_z\left(\frac{\Delta\omega T_p}{2}(1 - \varepsilon\Delta\omega)\right) \\
 &= R_y(\pi)R_x\left(\frac{\pi}{2}\right)R_z\left(\frac{\Delta\omega T_p}{2}(1 - \varepsilon\Delta\omega)\right). \tag{9}
 \end{aligned}$$

The first z -rotation commutes with the initial state, and the last y -rotation commutes with the final state; the central rotation delivers the desired outcome. We tested the prediction of Eq. [9] and found it to be quite accurate. Nevertheless, careful study turned up the following points: (1) the final delay is slightly longer than $\frac{T_p}{2}$, by perhaps one part in a thousand; (2) at the edges of the usable bandwidth the model begins to break down, and some small amount of x -magnetization is produced; (3) the sharpness of the transition edges is blurred slightly by the shorter HS $180_y^\circ(\frac{T_p}{2})$ pulse; (4) the excitation profile is no longer quite symmetric; (5) there seems to be a non-negligible loss of signal intensity even when all the pulses are calibrated carefully.

These observations are in accord with independent work by Böhlen *et al.* (32, 33) using constant-amplitude RF pulses with a linear frequency sweep. Following the same lines almost 10 years ago, and with the help of numerical simulation, they proposed sequences with the structure of P_1 but with two chirped pulses. Because chirp 180° pulses can show appreciably nonuniform inversion (25), it was important to use some phase cycling, described below, to improve the profile. Chirped pulses, while broadband, are not selective and so are not suitable for the applications envisaged here.

Figure 4 shows the experimental results of P_1 using a single transient. Even with no attempt to be more sophisticated, the results are surprisingly good. A simple improvement, along the lines of excitation sculpting, is to make sure to discard any new transverse magnetization produced by the HS 180° or any magnetization not properly refocused, and therefore automatically of wrong phase. This improvement can be implemented with either EXORCYCLE (32–34) or a small matched pair of pulsed field gradients flanking the HS 180° (or both). It affects the performance mostly near the edges of the bandwidth. Recovering a symmetrical profile is as easy as changing the algebraic sign of all the phases, $\varphi_k \rightarrow -\varphi_k$, in *all* the pulses, and co-adding the two results. This *phase reversal* is a very useful trick to employ, but for brevity we will not derive its properties here except to say that y - and z -magnetization will be symmetric, and x -magnetization will be antisymmetric, with respect to offset under this co-addition scheme. The overall phase of the pulse needs to be correctly adjusted, of course.

The scheme P_1 is a close cousin of the pure-phase 180° pulse described by Hwang *et al.* (35) that is made up of three HS 180° s, the outer two of which have half the pulsewidth of the

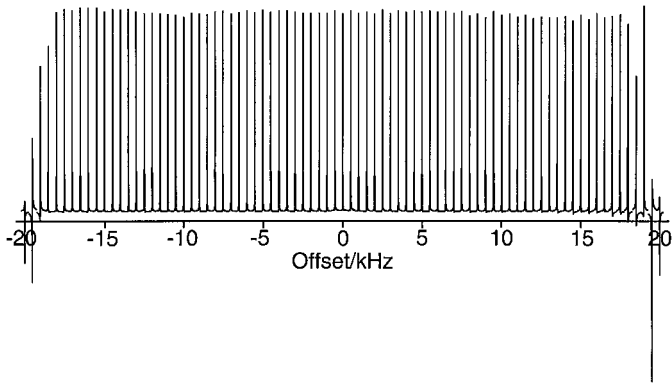


FIG. 4. The experimental offset dependence for the simple scheme P_1 , consisting of a 4.0-ms HS 90° followed immediately by a 2.0-ms HS 180° pulse and a delay of 2.0 ms plus 1.8 μ s. Instrumental delays having to do with commencement of the waveform memory were compensated with matching dummy statements on either side of the HS 180° element. The formulas in the text were used, digitizing the waveform in 1000 steps of 4 or 2 μ s, respectively. Only a single transient has been used, with no attempt to remove magnetization by phase cycling or gradients. While the profile is not exactly symmetric, it is still quite usable. A fairly substantial bandwidth of >37 kHz is achieved. The HS 90° pulse employed peak field of only 1.88 kHz, whereas the shorter and necessarily stronger HS 180° pulse required 7.98 kHz. The resonance line is the proton signal from the ASTM “2 Hz” H_2O sample, consisting of residual HDO in 99% D_2O , with $GdCl_3$ added to speed relaxation. It has been sampled every 0.5 kHz over ± 20 kHz with respect to exact resonance.

center one. Indeed, the simplified model introduced here makes the result of Ref. (35) transparent to derive. However, it also points out an insidious difficulty, shared by P_1 , the chirp pulses of Böhlen *et al.* (32, 33), and by the 3-pulse refocusing element (35). This difficulty is point (5) above, that there seems to be some loss of signal. The culprit is the RF inhomogeneity over the sample volume (33). That is, the simplified models are only decent for a thin spatial contour of the sample where the B_1 field is near the nominal value B_1^0 . Other magnetization has either the wrong phase, reduced amplitude, or both. The surprise is how pronounced the effect can be.

This effect can be framed in terms of the so-called Bloch–Siegert phase (BSP) (36, 37) that arises when an off-resonance pulse, for example a carbonyl decoupling pulse, is applied when other magnetization is transverse. Suppose a conventional selective rectangular 1.0 ms 180° pulse is applied. At an offset $\frac{\Delta\omega}{2\pi} = \frac{1}{2}\sqrt{3}$ kHz all magnetization undergoes a 360° trajectory, and so is returned to the same position it occupied when the selective pulse commenced. However, it *should* have acquired a phase $\Delta\omega T_p = \pi\sqrt{3}$ or 311.8° during this time. The magnetization differs from the correct position by 48.2° .

Now consider the BSP for the HS 180° pulse. The analysis is dissimilar because the pulse directly affects the spin we are considering. At the nominal condition, B_1^0 , the simple model of Fig. 3b works well, the pulse being phased so that it behaves as a 180° pulse. However, rather than just having an offset-

dependent delay on either side of perfect 180° pulse, we should include the BSP that accrues during the first part of the pulse, when an off-resonance field is applied, and that during the last part of the pulse when the same is true again. Although the sign of the effective field changes on either end of the sweep, the spin flips somewhere in the middle, too. As a result, these phase shifts do not cancel: if the pulse is phased to produce a 180° rotation on resonance at the nominal condition, then changing the RF level slightly could produce a phase shift. Accordingly, an improved model is represented in terms of rotation operators as follows:

$$R = R_z \left(\frac{\Delta\omega T_p}{2} (1 + \varepsilon \Delta\omega) \right) R_z \left(\delta \left(1 - \frac{B_1}{B_1^0} \right) \right) \\ \times R_y(\pi) R_{-z} \left(\delta \left(1 - \frac{B_1}{B_1^0} \right) \right) R_z \left(\frac{\Delta\omega T_p}{2} (1 - \varepsilon \Delta\omega) \right). \quad [10]$$

In an inhomogeneous field these variable phase shifts δ cause magnetization vectors to fan out, leading to a loss of signal. While Eq. [2] guarantees that these phase shifts cancel out if two matched inversion pulses are applied, for an odd number of inversion pulses, or for a single such pulse, there could be an irreparable loss of signal that depends on δ , which in turn depends on f_{max} and T_p .

Figure 5 shows that this loss could be significant. The figure shows the calculated amount of x - and y -magnetization produced, along with the relative phase shift, on resonance, as a function of the normalized field B_1/B_1^0 . A single 2-ms HS 180° with $f_{max} = 38$ kHz, $\gamma B_1^{peak}/2\pi = 7.98$ kHz (nominal) corresponding to $\kappa = 1.83$ in Eq. [7], and phased to produce no x -magnetization at the nominal condition on resonance, is used. The initial state is pure y -magnetization, $\langle I_y \rangle = -1$. Within an alarmingly narrow $\pm 10\%$ range in B_1/B_1^0 there is a $\pm 90^\circ$ phase shift; i.e., $\langle I_x \rangle = \pm 1$! The nearly sinusoidal dependence of the magnetization (linear phase shift) as the field is increased, a region where the inversion pulse is surely inverting properly, is the fingerprint of the unwanted BSP. Unfortunately, the magnitude of this BSP is not even approximately canceled by any similar effect during the first HS 90° pulse. In fact the phase shifts from the first pulse, while nonzero, are relatively minor because the applied field is much weaker, and there is no detectable BSP operating over roughly the first half of the HS 90° pulse, during which time magnetization resides mostly along the z -axis. Accordingly, we must deliberately compensate for the BSP, while maintaining the phase properties with respect to offset.

This is easily accomplished by replacing the HS 180° in P_1 with a new HS 180° having the same $f_{max} = 38$ kHz but the *same* length as the HS 90° , rather than half the length. The same delay then takes care of the linear phase roll with respect to offset, and a quadratic phase roll of opposite sense is introduced.

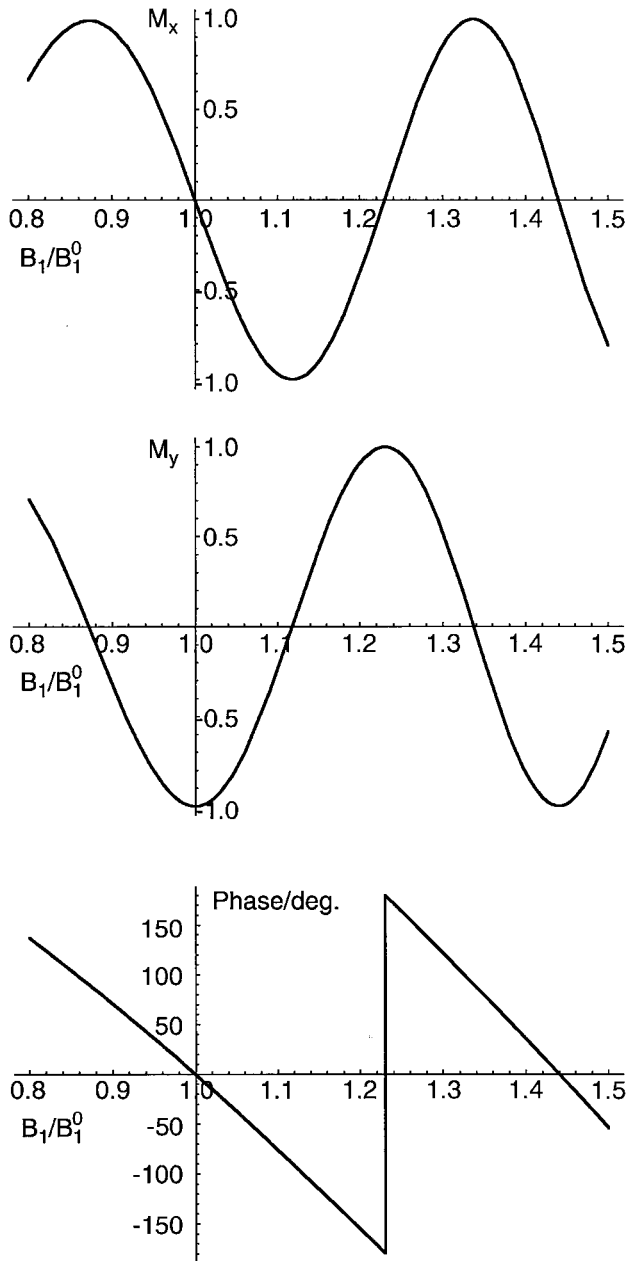


FIG. 5. An illustration of the “Bloch–Siegert phase” displayed by HS 180° pulses. The upper traces show the calculated x - (quadrature phase) and y - (in phase) magnetization produced by a 2.0-ms HS 180° pulse, identical to the second pulse used to produce Fig. 4. The bottom trace shows the relative phase shift. All are plotted as a function of the B_1 field, expressed as a fraction of the nominal field, B_1^0 . With only a relatively small fractional change in the field, a substantial phase shift is observed. In most high-resolution probes there can be a $\pm 10\%$ range of fields over the active sample volume. In such a case, the integrated signal shows some noticeable attenuation due to the variable phase shifts in different spatial regions. Using a matched pair of 180° pulses completely removes the unwanted phase shift.

This quadratic roll is then removed by the final HS 180° pulse, which is once again half the length of the HS 90° pulse. The whole sequence is thus $P_2 = \text{HS } 90_x^\circ(T_p) - \text{HS } 180_y^\circ(T_p) - \frac{T_p}{2} - \text{HS } 180_y^\circ(\frac{T_p}{2})$ which, neglecting the BSP, can be analyzed

as Eq. [9]:

$$\begin{aligned}
 P_2 &= R_z\left(\frac{\Delta\omega T_p}{4}(1 + \varepsilon\Delta\omega)\right)R_y(\pi)R_z\left(\frac{\Delta\omega T_p}{4}(1 - \varepsilon\Delta\omega)\right) \\
 &\times R_z\left(\frac{\Delta\omega T_p}{2}\right)R_z\left(\frac{\Delta\omega T_p}{2}(1 + \varepsilon\Delta\omega)\right) \\
 &\times R_y(\pi)R_z\left(\frac{\Delta\omega T_p}{2}(1 - \varepsilon\Delta\omega)\right) \\
 &\times R_z\left(\frac{\Delta\omega T_p}{2}(1 + \varepsilon\Delta\omega)\right)R_x\left(\frac{\pi}{2}\right)R_z\left(\frac{\Delta\omega T_p}{2}(1 - \varepsilon\Delta\omega)\right) \\
 &= R_y(2\pi)R_x\left(\frac{\pi}{2}\right)R_z\left(\frac{\Delta\omega T_p}{2}(1 - \varepsilon\Delta\omega)\right). \quad [10]
 \end{aligned}$$

The models clearly predict that, in general, the only requirement to approximately compensate for the quadratic phase roll of the HS 90° pulse is to mismatch the lengths of the two HS 180°s by half the length of the HS 90°. The HS 180° immediately following the HS 90° is always the longer of the two. Thus, we can view P_1 as a limiting case of P_2 in which the second HS 180° has been reduced all the way to zero length. It is possible to use longer HS 180°s, e.g., 5 and 3 ms, 7 and 5 ms, with similar results. This also lowers the peak power requirement in accordance with Eq. [7]. Due to the different transition-region performance, which depends only on the actual pulsewidth, these sequences differ in detail at the edges of the passband. As Eq. [2] guarantees that the BSP is canceled when the two HS 180°s are identical, by continuity it follows that the BSP will be small when they are closely-enough matched in length. It turns out that they need not be too close in percentage terms because the stronger RF field of the shorter pulse partially offsets the decrease in pulsewidth. That is, P_2 already works well. It can be improved by slightly bumping up the intensity of the second HS 180°, by about 0.5 dB for the exact conditions used in Fig. 6, a finesse that begins to counter the slight BSP of the HS 90° as well.

Figure 6 shows experimental results, under these conditions, obtained with P_2 , with a single transient (top). The bottom trace is obtained with independent EXORCYCLE phase cycling of each of the refocusing pulses, along with co-addition of a phase-reversed sequence. This 32-step phase cycle can be reduced to just two transients if PFGs are used, or if the exact performance in the transition region is not crucial. If perfect symmetry of the passband is unimportant, then a single transient clearly suffices. These results would be interesting even if the bandwidth were not adjustable at will, so the latter emerges as a pleasant bonus of the sequence.

With regard to the nettlesome BSP, Fig. 7 demonstrates the phase stability of P_2 that should be observed on resonance, by numerical calculation. The large linear phase roll of Fig. 5 has been converted into a relatively small quadratic one. A single transient has been assumed, but the results neither hinge on the number of transients, nor on the exact offset chosen. The stability

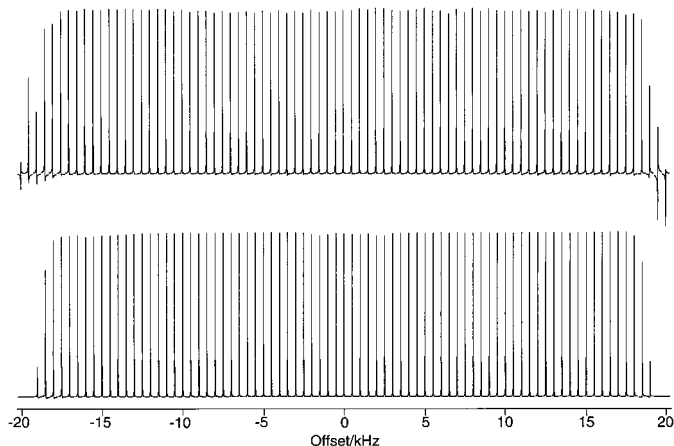


FIG. 6. Experimental demonstration of the sequence P_2 , consisting of a 4.0-ms HS 90° followed immediately by a 4.0-ms HS 180° pulse and a delay of 2.0 ms plus $1.8 \mu\text{s}$, and then a 2.0-ms HS 180° pulse. Instrumental delays having to do with commencement of the waveform memory were compensated with matching dummy statements on either side of the HS 180° element. All pulses used $f_{\text{max}} = 38 \text{ kHz}$ and with peak RF fields of 1.88 kHz, 5.64 kHz, and 8.41 kHz, respectively. The slight increase, from 7.98 kHz ($\kappa = 1.83$) to 8.41 kHz ($\kappa = 1.93$) for the last pulse improves the stability of the whole sequence with respect to changes in B_1/B_1^0 , as discussed in the text. Note that slightly longer HS 180° 's could be used, thereby lowering the peak field requirement for these pulses at the expense of the overall duration. Top: results of a single transient, no phase cycling. Bottom: results of 32 transients, using EXORCYCLE on each of the refocusing pulses, and a co-added phase-reversed sequence. A pleasing pure-phase symmetrical profile is obtained. Identical results were obtained using 200- μs PFGs instead of the EXORCYCLE, using only two transients (data not shown).

holds at all offsets over which the pulse operates well. Finally Fig. 8 shows an experimental comparison between P_1 and P_2 over a $\pm 15\%$ change in the nominal field. Clearly there is a huge improvement by accounting for the BSP. The very slight phase roll in P_2 is in fact somewhat smaller than predicted by simulation, apparently because the distribution of actual values partially averages the profile of Fig. 7 and the average shows less range than the individual values do.

The intrinsic sensitivity of both P_1 and P_2 to RF inhomogeneity, aside from any BSP problems, resides solely with the first HS 90° pulse. This pulse is not adiabatic, and shows no particular compensation, in terms of residual z -magnetization, for instance, with respect to changes in B_1/B_1^0 . However, P_2 performs similarly to a conventional 90° pulse in this regard, the majority of the signal being transformed into y -magnetization even with appreciable miscalibration. Over a $\pm 10\%$ range in B_1/B_1^0 , $\sim 99\%$ of the expected signal is obtained. For most high-resolution applications, further compensating the excitation pulse is not required, and will not lead to major gains in sensitivity.

In conclusion, by a somewhat circuitous means we have introduced what we believe is the first example of adjustable, broadband, uniform-phase selective excitation. To simplify the analysis, we have employed very useful approximate models to replace the complicated behavior of the actual FM pulses. These

models have clarified, quantified, and explained the behavior with respect to resonance offset and RF amplitude. The HS 180° pulses show mostly quadratic phase shifts with respect to offset, and mostly linear phase shifts with respect to B_1/B_1^0 . The HS 90° shows qualitatively similar behavior, with an additional large linear term in offset of close to half the pulsewidth. The models are most applicable in the far field limit, where the FM pulse behaves completely differently than does a conventional fixed-phase pulse. We have illustrated the salient features of the FM 90° and the “mismatched double echo” by employing the hyperbolic secant family, but the insight and machinery applies more broadly. We note in passing that related transformations such as $I_y \rightarrow -I_z$ can be formed easily, allowing almost all multidimensional NMR experiments to be carried out with these new schemes. The slightly roundabout route used to arrive at the selective excitation scheme suggested the acronym ABSTRUSE: *A*dustable, *B*roadband, *S*ech/*T*anh-*R*otation *U*niform *S*elective *E*xcitation. At high field, where even a conventional 90° pulse begins to show deficiencies, there could be a substantial advantage to ABSTRUSE pulse sequences. While we have not attempted to optimize these sequences with respect to total duration, focusing on their conceptual underpinnings instead,

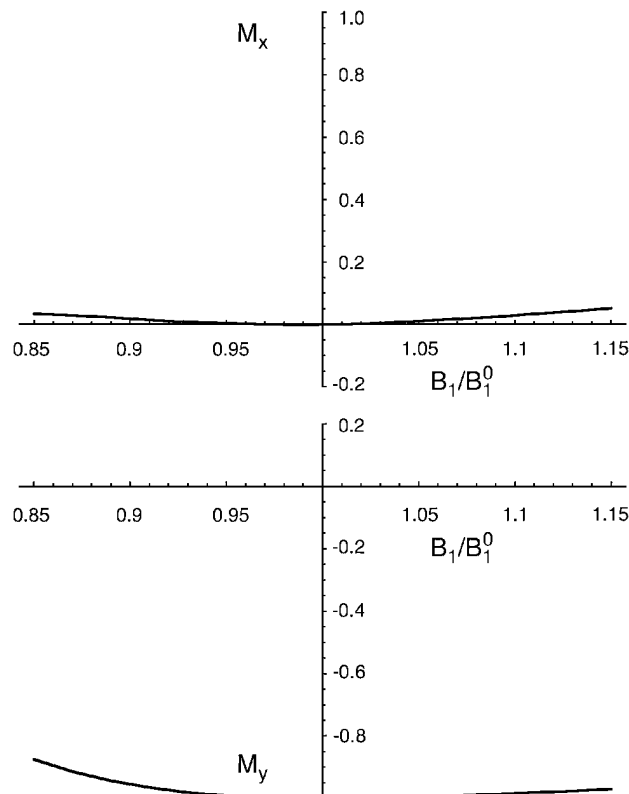


FIG. 7. Calculated x - and y -magnetization for the ABSTRUSE scheme P_2 as a function of the normalized field B_1/B_1^0 . There is greatly improved stability in the phase of the magnetization compared with the results of Fig. 5, which closely resemble that obtained with the simpler scheme P_1 . A single slice corresponding to the on-resonance case has been computed, but the phase stability is not strongly offset-dependent, so the results are representative.

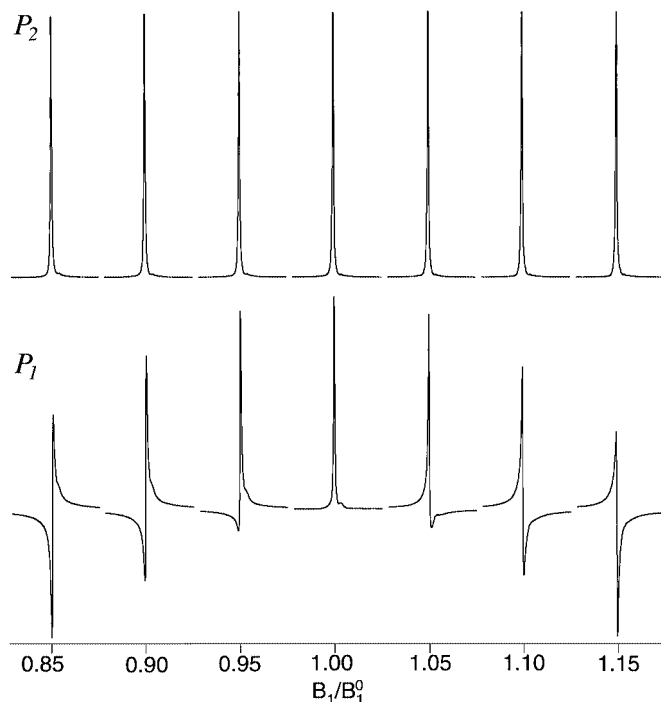


FIG. 8. Experimental results corresponding to the calculation of Fig. 7. Top: the ABSTRUSE scheme, P_2 . Bottom: the simpler scheme, P_1 . The predicted phase stability or instability is observed in practice. A single slice corresponding to the on-resonance case has been measured in each case, over a $\pm 15\%$ range in B_1/B_1^0 , by incrementing the fine power attenuator controlling the waveform amplitude. The phase is also stable at all other offsets where the pulse performs well. The phase stability of the waveform generator electronics over this range was independently checked, using a single unmodulated pulse, and found to be essentially flawless. The ABSTRUSE pulse appears to work a little better in practice than in theory due to the observed signal itself being averaged over a spread in B_1/B_1^0 values. The spectra are on the same absolute scale. A single transient has been acquired for each.

the described sequences are an excellent beachhead for a detailed numerical campaign. There are obvious implications for slice-selection in the presence of a gradient, and other imaging applications, as well. In some cases the selective passband requirement can be relaxed, in which case interesting new possibilities for high-power broadband sequences emerge. We will describe these and related aspects in future publications.

ACKNOWLEDGMENT

This work was supported by the National Science Foundation, CHE-9900422.

REFERENCES

1. M. H. Levitt and R. Freeman, Compensation for pulse imperfections in NMR spin-echo experiments, *J. Magn. Reson.* **43**, 65–80 (1981).
2. R. Freeman, S. P. Kempell, and M. H. Levitt, Radiofrequency pulse sequences which compensate their own imperfections, *J. Magn. Reson.* **38**, 453–479 (1980).
3. M. H. Levitt and R. Freeman, Composite pulse decoupling, *J. Magn. Reson.* **43**, 502–507 (1981).
4. A. J. Shaka, J. Keeler, and R. Freeman, Evaluation of a new broadband decoupling sequence: WALTZ-16, *J. Magn. Reson.* **53**, 313–340 (1983).
5. M. H. Levitt and R. R. Ernst, Composite pulses constructed by a recursive expansion procedure, *J. Magn. Reson.* **55**, 247–254 (1983).
6. A. J. Shaka and R. Freeman, Composite pulses with dual compensation, *J. Magn. Reson.* **55**, 487–493 (1983).
7. C. Bauer, R. Freeman, T. Frenkiel, J. Keeler, and A. J. Shaka, Gaussian pulses, *J. Magn. Reson.* **58**, 442–457 (1984).
8. A. J. Shaka, Composite pulses for ultra-broadband spin inversion, *Chem. Phys. Lett.* **120**, 201–205 (1985).
9. R. Tycko, H. M. Cho, E. Schneider, and A. Pines, Composite pulses without phase distortion, *J. Magn. Reson.* **61**, 90–101 (1985).
10. L. Emsley and G. Bodenhausen, Gaussian pulse cascades: New analytical functions for rectangular selective inversion and in-phase excitation in NMR, *Chem. Phys. Lett.* **165**, 469–476 (1990).
11. H. Geen and R. Freeman, Band-selective radiofrequency pulses, *J. Magn. Reson.* **93**, 93–141 (1991).
12. M. Garwood and Y. Ke, Symmetric pulses to induce arbitrary flip angles with compensation for RF inhomogeneity and resonance offsets, *J. Magn. Reson.* **94**, 511–525 (1991).
13. T.-L. Hwang and A. J. Shaka, Water suppression that works: Excitation sculpting using arbitrary waveforms and pulsed field gradients, *J. Magn. Reson. Series A* **112**, 275–279 (1995).
14. K. Stott, J. Stonehouse, J. Keeler, T.-L. Hwang, and A. J. Shaka, Excitation sculpting in high-resolution nuclear magnetic resonance spectroscopy: Application to selective NOE experiments, *J. Am. Chem. Soc.* **117**, 4199–4200 (1995).
15. A. J. Shaka and R. Freeman, “Prepulses” for spatial localization, *J. Magn. Reson.* **64**, 145–150 (1985).
16. L. Allen and J. H. Eberly, “Optical Resonance and Two-Level Atoms,” pp. 101–107, Wiley, New York (1975).
17. J. Baum, R. Tycko, and A. Pines, Broadband population inversion by phase modulated pulses, *J. Chem. Phys.* **79**, 4643–4644 (1983).
18. J. Baum, R. Tycko, and A. Pines, Broadband and adiabatic inversion of a two-level system by phase-modulated pulses, *Phys. Rev. A* **32**, 3435–3447 (1985).
19. M. S. Silver, R. I. Joseph, and D. I. Hoult, Selective spin inversion in nuclear magnetic resonance and coherent optics through an exact solution of the Bloch–Riccati equation, *Phys. Rev. A* **31**, 2753–5 (1985).
20. M. R. Bendall, Broadband and narrowband spin decoupling using adiabatic spin flips, *J. Magn. Reson. Series A* **112**, 126–129 (1995).
21. E. Kupce and R. Freeman, Optimized adiabatic pulses for wideband spin inversion, *J. Magn. Reson. Series A* **118**, 299–303 (1996).
22. A. Tannús and M. Garwood, Improved performance of frequency-swept pulses using offset-independent adiabaticity, *J. Magn. Reson. Series A* **120**, 133–137 (1996).
23. A. Abragam, “The Principles of Nuclear Magnetism,” pp. 34–36, Oxford Univ. Press, Oxford (1961).
24. S. Conolly, G. Glover, D. Nishimura, and A. Macovski, A reduced power selective adiabatic spin-echo pulse sequence, *Magn. Reson. Med.* **18**, 28–38 (1991).
25. M. A. Smith, H. Hu, and A. J. Shaka, Improved broadband inversion performance for NMR in liquids, *J. Magn. Reson.* **151**, 269–283 (2001).
26. Y. Luo, R. A. de Graaf, L. DelaBarre, A. Tannús, and M. Garwood, BISTRO: An outer-volume suppression method that tolerates RF field inhomogeneity, *Magn. Reson. Med.* **45**, 1095–1102 (2001).
27. B. A. Jacobsohn and R. K. Wangsness, Shapes of nuclear induction signals, *Phys. Rev.* **73**, 942–946 (1948).

28. R. Tycko, A. Pines, and J. Guckenheimer, Fixed point theory of iterative excitation schemes in NMR, *J. Chem. Phys.* **83**, 2775–2802 (1985).
29. E. Kupce and R. Freeman, Compensation for spin–spin coupling effects during adiabatic pulses, *J. Magn. Reson.* **127**, 36–48 (1997).
30. C. Zwanen, S. J. F. Vincent, and L. E. Kay, Analytical description of the effect of adiabatic pulses on IS, I₂S, and I₂S spin systems, *J. Magn. Reson.* **130**, 169–175 (1998).
31. K. Hallenga and G. M. Lippens, A constant-time ¹³C–¹H HSQC with uniform excitation over the complete ¹³C chemical shift range, *J. Biomol. NMR* **5**, 59–66 (1995).
32. J.-M. Böhlen, M. Rey, and G. Bodenhausen, Refocusing with chirped pulses for broadband excitation without phase dispersion, *J. Magn. Reson.* **84**, 191–197 (1989).
33. J.-M. Böhlen and G. Bodenhausen, Experimental aspects of chirp NMR spectroscopy, *J. Magn. Reson. Series A* **102**, 293–301 (1993).
34. G. Bodenhausen, R. Freeman, and D. L. Turner, Suppression of artifacts in two-dimensional J spectroscopy, *J. Magn. Reson.* **27**, 511–514 (1977).
35. T.-L. Hwang, P. C. M. Van Zijl, and M. Garwood, Broadband adiabatic refocusing without phase distortion, *J. Magn. Reson.* **124**, 250–254 (1997).
36. L. Emsley and G. Bodenhausen, Phase shifts induced by transient Bloch–Siegert effects in NMR, *Chem. Phys. Lett.* **168**, 297–303 (1990).
37. M. Sattler, J. Schleucher, and C. Griesinger, Heteronuclear multidimensional NMR experiments for the structure determination of proteins in solution employing pulsed field gradients, *Prog. NMR Spectros.* **34**, 93–158 (1999).